



## QUANTIFICATION OF THIOACETAMIDE-INDUCED LIVER NECROSIS USING FRACTAL ANALYSIS

### *KVANTIFIKACIJA TIOACETAMIDOM INDUKOVANE NEKROZE JETRE POMOCU FRAKTALNE ANALIZE*

Jovan Milosavljević<sup>1</sup>, Ivan Zaletel<sup>2</sup>, Nela Puškaš<sup>2</sup>

<sup>1</sup> University of Belgrade, Faculty of Medicine, Belgrade, Serbia

<sup>2</sup> University of Belgrade, Faculty of Medicine, Institute of Histology and Embryology, Belgrade, Serbia

**Correspondence:** milosavljevic.jov@gmail.com

#### Abstract

**Introduction:** The liver is particularly susceptible to the toxicity from numerous chemical agents, because of its central role in the detoxification. Thioacetamide-induced liver injury is used as an animal model of acute hepatic failure. Fractal analysis is a mathematical method used to measure the complexity of natural objects and can be represented solely using one parameter – the fractal dimension.

**Aim:** The aim of this study was to investigate whether fractal analysis could be used to determine and quantify the hepatotoxic effect of thioacetamide on rat liver.

**Material and methods:** Adult male Wistar rats were randomized into two groups: experimental group undergoing treatment with thioacetamide (600 mg/kg i.p.) and control group undergoing treatment with saline. Tissue samples were stained with hematoxylin & eosin (H&E) and Masson's trichrome protocol. Graphic processing and fractal analysis were performed using the ImageJ software. Two fractal dimensions were calculated: the fractal dimension of liver parenchyma (Dpar) and the fractal dimension of liver sinusoids (Dsin).

**Results:** Dpar value was significantly lower in the experimental group, as compared to the control, both samples stained with H&E and Masson's trichrome ( $p < 0.0001$ ). Dsin value was significantly higher in the experimental group, in tissue samples stained with H/E ( $p < 0.0001$ ). Additionally, we calculated the Dpar/Dsin ratio, which was significantly lower in the experimental group, in tissue samples stained with both H&E and Masson's trichrome protocol.

**Conclusion:** These results show that fractal analysis could prove as a useful, easy and low-cost method in the detection and quantification of thioacetamide-induced liver necrosis.

#### Keywords:

hepatic encephalopathy,  
toxicity,  
liver lobule,  
box-counting



## Sažetak

**Uvod:** Jetra je posebno podložna oštećenju koje nastaje toksičnim dejstvom brojnih supstanci budući da predstavlja glavni organ koji učestvuje u detoksikaciji. Tioacetamid (TAA) se koristi kao animalni model za ispitivanje akutnog oštećenja jetre. Fraktalna analiza je matematički metod kojim se meri kompleksnost prirodnih objekata i može se iskazati jednim parametrom – fraktalnom dimenzijom.

**Cilj:** Cilj ovog rada bilo je ispitivanje da li fraktalna analiza može da se koristi za procenu hepatotoksičnog efekta TAA na tkivo jetre pacova.

**Materijal i metode:** Odrasli mužjaci pacova Vistar (Wistar) soja podeljeni su u dve grupe - eksperimentalnu, koja je tretirana TAA u dozi od 600 mg/kg i kontrolnu, koja je tretirana fiziološkim rastvorom. Uzorci tkiva jetre bojeni su tehnikama hematoksilin/eozin (H/E) i Mason (Masson) trihrom. Obrada fotografija i fraktalna analiza rađene su u programu ImageJ. Izračunavane su fraktalna dimenzija parenhima (Dpar) i fraktalna dimenzija sinusoida jetrinih lobulusa (Dsin).

**Rezultati:** Srednja vrednost Dpar bila je statistički značajno niža u eksperimentalnoj u odnosu na kontrolnu grupu, na uzorcima bojenim H/E tehnikom i Mason trihromnom metodom ( $p < 0,0001$ ). Srednja vrednost Dsin pokazala je statistički značajno veću vrednost u eksperimentalnoj u odnosu na kontrolnu grupu na uzorcima tkiva bojenim tehnikom H/E ( $p < 0,0001$ ). Dodatno smo izračunali Dpar/Dsin odnos, koji je statistički značajno niži u eksperimentalnoj grupi na uzorcima bojenim H/E tehnikom i Mason trihromnom metodom.

**Zaključak:** Rezultati ove studije pokazuju da se fraktalna analiza pokazala kao koristan metod u cilju kvantifikovanja oštećenja tkiva jetre tioacetamidom.

### Ključne reči:

hepatična encefalopatija,  
toksičnost,  
lobulus jetre,  
box-counting

## Introduction

The liver plays a central role in the detoxification and therefore is particularly susceptible to damage, due to toxic properties of numerous chemical agents (therapeutic or environmental). Hepatotoxicity can be classified as intrinsic (predictable, dose-dependent) and idiosyncratic (unpredictable, dose-independent) (1). Liver injury may result from direct toxicity, indirectly through bio activation processes, or it can be immunologically mediated (2). Hepatotoxins initially induce damage in the centrilobular areas of the liver, where high levels of CYP450 oxidases are expressed. Through CYP450 enzyme system xenobiotic are converted to active toxins, followed by the production of reactive oxygen species (ROS), lipid peroxidation and the release of pro-inflammatory cytokines (3).

Toxin-induced liver injury can range from asymptomatic and mild, to acute liver failure and chronic liver disease (1, 2). Acute liver failure is defined as an acute liver illness associated with encephalopathy and coagulopathy (4), and it is caused by massive hepatic necrosis, most often induced by drugs or toxins (5). With the loss of liver detoxification function, the levels of toxic substances rise in the plasma, such as ammonia. High levels of ammonia are associated with hepatic encephalopathy (HE), a severe neuropsychiatric syndrome (6). Thioacetamide (TAA) is a substance commonly used to induce a model of acute liver failure, as well as HE in rats (7–9). TAA causes hepatocellular necrosis after biotransformation to an active metabolite and by generating ROS (3).

Fractal analysis is a useful method of measuring the complexity of natural objects. Through the use of frac-

tal dimension, it is possible to quantify the irregularity and complexity of structures in biological systems (10). It is widely used in many different areas of biomedical sciences, such as neurosciences (11–13), tumor and liver pathology (14–16) and many other areas where the use of image analysis is necessary (17, 18).

However, we found no reports on using fractal analysis for the estimation and the quantification of hepatotoxic tissue changes. Thus, this study aimed to investigate whether fractal analysis could be used for the quantitative analysis of hepatotoxic necrosis, induced by TAA.

## Material and Methods

### Experimental animals

The study was carried out on adult male Wistar rats (weight 170 - 200 g). All animals were housed individually in a controlled environment (temperature of  $22 \pm 1$  °C, relative humidity of 50%, with a 12/12 h light/dark cycle). Food and water were provided ad libitum. All of the experimental procedures were in accordance with the Directive of the European Parliament (2010/63/EU) and were approved by the Ethics Committee of the University of Belgrade (Permission No. 1891/2).

Animals were randomized into two groups: the experimental group, undergoing treatment with TAA ( $n = 3$ ), and the control group, undergoing treatment with saline ( $n = 3$ ). TAA (Sigma Aldrich) was dissolved in saline (0.9% NaCl) and injected intraperitoneally in two doses of 300 mg/kg, within a period of 24 h. This dose has been chosen, since it has been shown in our previous studies it causes acute moderate HE in rats, with decline in motor

activity and EEG changes that predominantly correlate with stage II HE in humans (19, 20). All of the animals were sacrificed 24 h after the last dose of TAA.

### Tissue preparation and image acquisition

Liver specimens from each group were collected from animals immediately after their sacrifice and fixed in 4% buffered formaldehyde solution. After embedding in paraffin, tissue samples were sectioned and stained with hematoxylin and eosin (H&E) and Masson's trichrome stain by a standard procedure.

Digital photographs of classical liver lobules were taken with the Leica DM4000 B LED microscope and the Leica Application Suite (LAS, v4.4.0) software at x200 magnification. The images were saved in TIFF format, with the dimensions of 2048 x 1536 pixels, resolution of 300 DPI and bit depth of 24. In order to avoid the differences between tissue sections, only the images of classical liver lobules where the terminal hepatic venule lies centrally (i.e. central vein), were used for further analysis. Thus, all of the obtained results refer to the changes that are present in the classical hepatic lobule. A total of 163 images were included in the study, of which 86 were from the experimental group (H&E – 36 and Masson's trichrome – 50) and 77 from the control group (H&E – 34 and Masson's trichrome – 43). Further image processing and fractal analysis were carried out in the ImageJ 1.48v software

(NIH, Bethesda, USA; free download from <http://rsbweb.nih.gov/ij/>).

### Fractal analysis

Two values of fractal dimension were calculated in each group of analyzed images: the fractal dimension of the liver lobule parenchyma ( $D_{par}$ ) and the fractal dimension of liver lobule sinusoids ( $D_{sin}$ ). In order to calculate  $D_{par}$ , digital photographs were converted to a binary format. The same procedure was used to calculate  $D_{sin}$  but with the addition of the invert command to the binarization process (**Figure 1** and **Figure 2**).

In this research, the fractal dimension of liver parenchyma and sinusoids was calculated using the box-counting method, where a grid of square cells (boxes, with cell size  $r$ ) is superimposed over the binary image. The total number of square boxes  $N(r)$  intersecting with the liver parenchyma is counted. This step is repeated with different cell sizes  $r$  and thus the fractal dimension is calculated as an absolute value of the slope of the log-log relationship between  $N(r)$  and  $r$  (21) (**Figure 3**). Default box sizes for counting the fractal dimension using the ImageJ software are 2, 3, 4, 6, 8, 12, 16, 32, 64. The box sizes used in this research were 1, 2, 4, 8, 16, 32, 64, 128, 256, 512, 1024, 2048 which were obtained as an increasing geometric progression  $2^n$  where  $n = 0, 1, 2 \dots 11$ , as also used in previous papers (11, 12). 2.4.

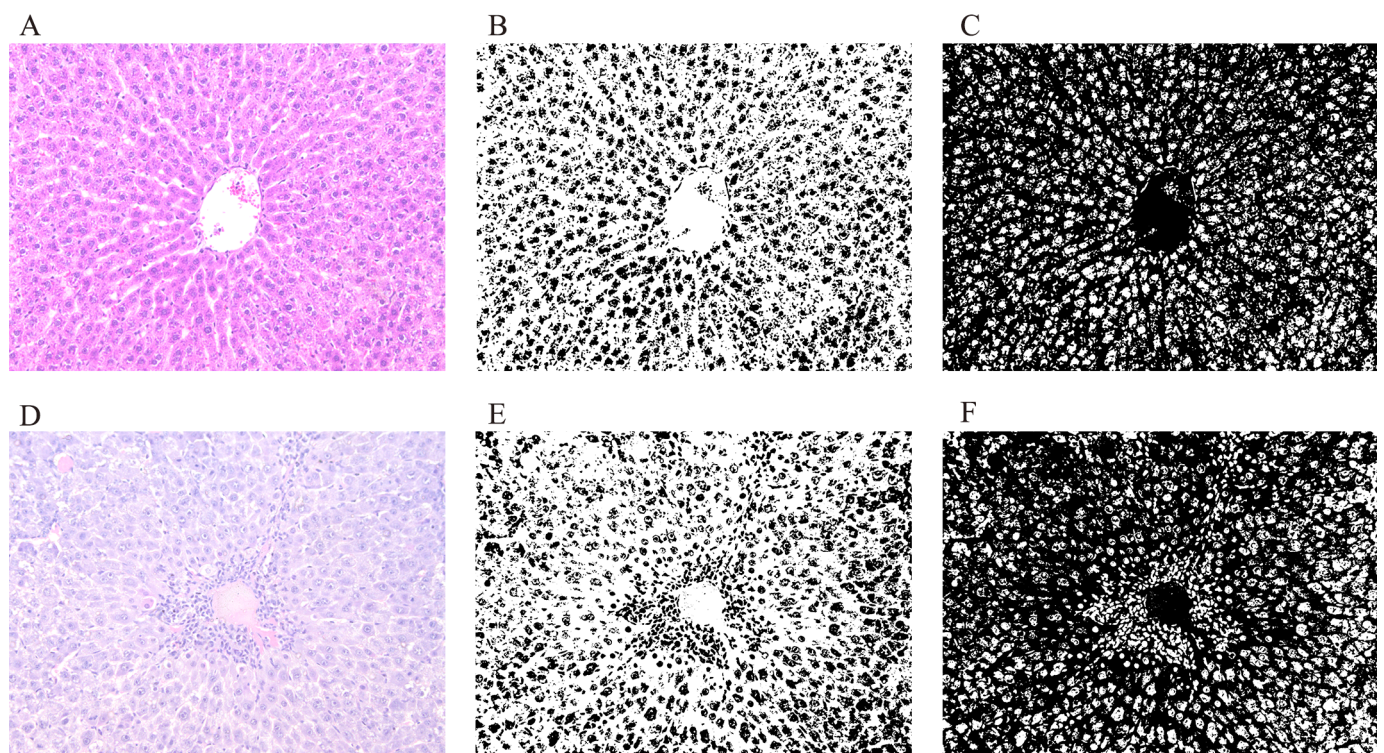


**Figure 1.** Steps in graphic processing of the classical liver lobule stained with H&E (original magnification x200). (A) Digital photograph of the liver lobule from the control group. (B) Binary image of the liver lobule parenchyma and (C) binary image of the liver lobule sinusoids. (D) Digital photograph of the liver lobule from the experimental group and binary images of lobule (E) parenchyma and (F) sinusoids. Scale bar = 100  $\mu$ m.

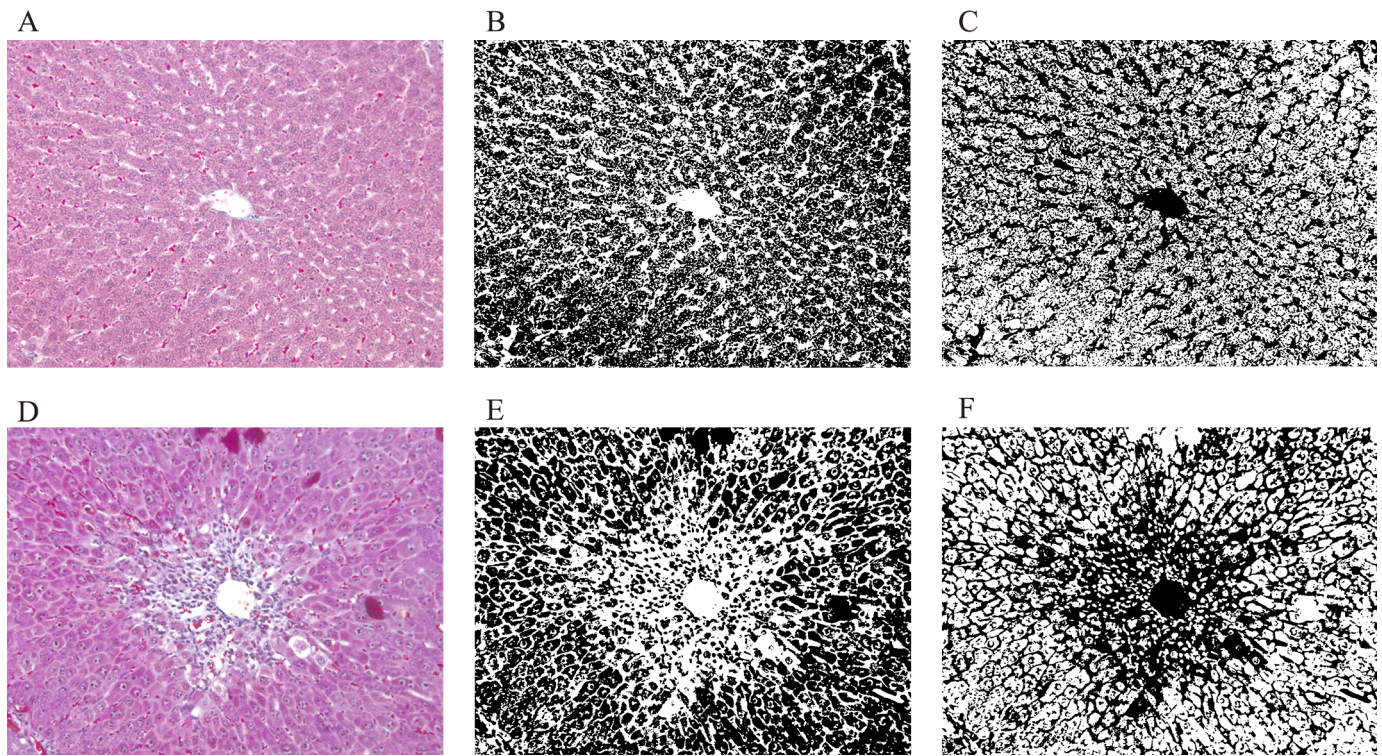


**Figure 2.** Steps in graphic processing of the classical liver lobule stained with Masson's trichrome method (original magnification x200). (A) Digital photograph of the liver lobule from the control group. (B) Binary image of the liver lobule parenchyma and (C) binary image of the liver lobule sinusoids. (D) Digital photograph of the liver lobule from the experimental group and binary images of lobule (E) parenchyma and (F) sinusoids. Scale bar = 100  $\mu\text{m}$ .

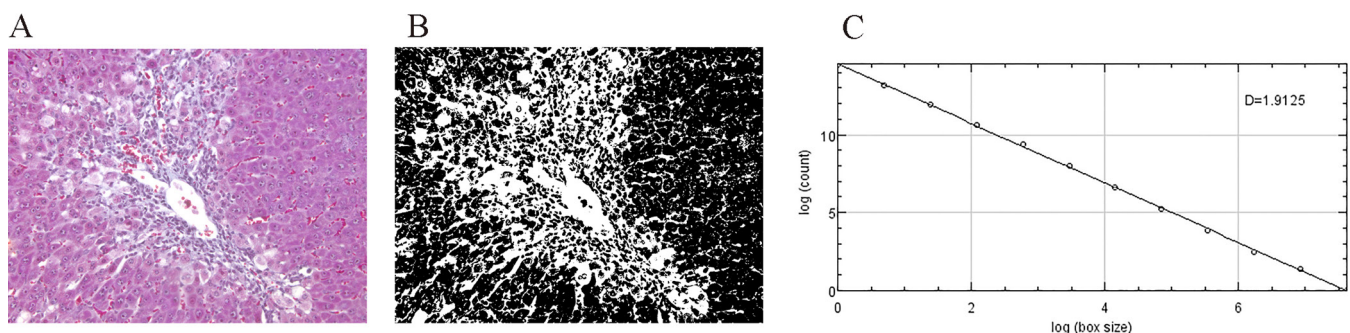


**Figure 3.** Steps in fractal analysis. (A) Digital photo of the classical liver lobule stained with Masson's trichrome was transformed into (B) the binary image on which the box-counting method was performed. (C) Log-log graph of the number of boxes and box sizes. The slope of the regression line corresponds to the fractal dimension  $D$ . Scale bar = 100  $\mu\text{m}$ .

### Statistical analysis

Normal distribution of data were tested by D'Agostino-Pearson omnibus normality test and Shapiro-Wilk normality test. The differences between the two groups were tested using Mann-Whitney's  $U$  test. The results are represented as median, with interquartile range. For  $p$  values less than 0.05, the differences between the groups were considered statistically significant.

### Results

The fractal analysis of liver parenchyma showed that  $D_{\text{par}}$  value was significantly lower in the experimental group, as compared to the control group, both samples

stained with H&E ( $U = 144.0$ ,  $p < 0.0001$ ) and Masson's trichrome ( $U = 275.0$ ,  $p < 0.0001$ ) (**Figure 4A**).

$D_{\text{sin}}$  value was significantly higher in the experimental group, comparing to the control group, in tissue samples stained with H&E ( $U = 262.0$ ,  $p < 0.0001$ ). Although, there was no statistically significant difference between  $D_{\text{sin}}$  values in the samples stained with Masson's trichrome ( $U = 823.0$ ,  $p = 0.052$ ), the TAA treated group showed higher values of fractal dimension, when compared to the control group (**Figure 4B**).

Additionally, we calculated the  $D_{\text{par}}/D_{\text{sin}}$  ratio, which was significantly lower in the experimental group, in tissue samples stained with both H&E ( $U = 162.0$ ,  $p < 0.0001$ ) and Masson's trichrome ( $U = 663.0$ ,  $p < 0.01$ ) (**Figure 4C**).

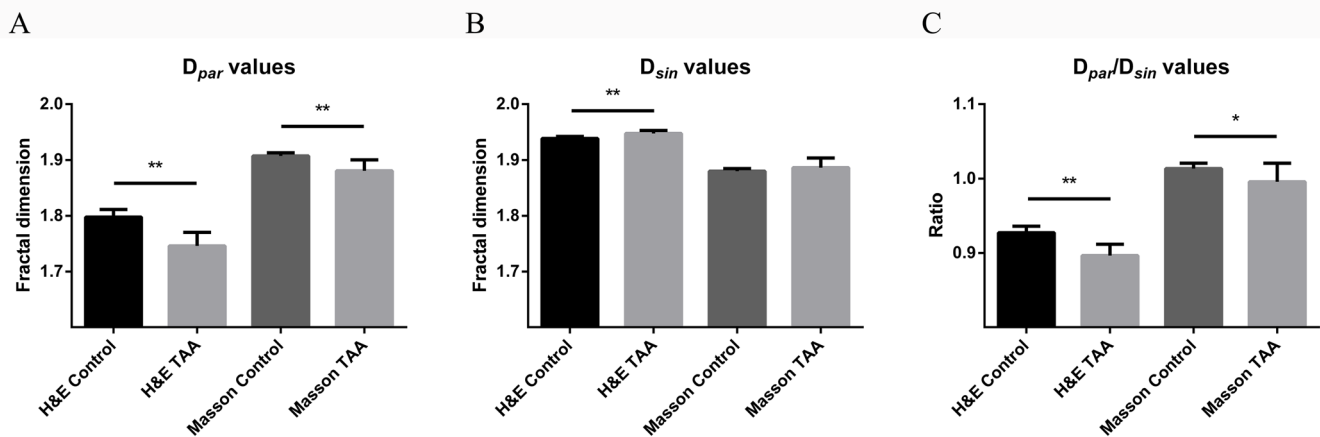


**Figure 4.** Fractal dimension of the liver lobule parenchyma and sinusoids in H&E and Masson trichrome stained sections. (A) Fractal dimension of the liver lobule parenchyma ( $D_{par}$ ). (B) Fractal dimension of the liver lobule sinusoids ( $D_{sin}$ ). (C) Ratio of fractal dimension of liver lobule parenchyma and fractal dimension of liver lobule sinusoids ( $D_{par}/D_{sin}$ ). Results are represented as median with interquartile range. Asterisk: \* - statistical significance  $< 0.01$ ; \*\* - statistical significance  $< 0.0001$

## Discussion

In fractal analysis, a type of quantitative analysis derived from fractal geometry (21, 22, 23), the complexity of analyzed structures can be represented solely using one parameter – the fractal dimension (23–25). Moreover, fractal dimension can characterize the shape of natural structures, more precisely than traditional morphometric measures, and it is now accepted as being more useful for the quantification of complex structures (26).

At the present time, fractal geometry is being used in diverse research areas, and is proving to be an increasingly beneficial tool. Previous studies have shown that fractal analysis can be used for the quantification of liver fibrosis with high level of diagnostic accuracy (14, 15). Fractal dimension represents a parameter that measures the complexity of tissue microarchitecture and it has been used for detection of morphological changes in cirrhotic liver (27), discrimination between different types of neoplastic and non-neoplastic liver tissue (28) and for age-related chromatin changes in normal hepatocytes (29). An increase in the fractal dimension is a typical characteristic of neoplastic tissue transformation (16, 30), due to infiltrative growth of malignant tumors, which increases tumor shape complexity (10). On the other hand, aging is associated with a decrease in nuclear size and chromatin complexity, which are responsible for a decline of nuclear fractal dimension of aged hepatocytes (29). Additionally, a decrease in fractal dimension due to loss of tissue complexity, uniformity and structure regularity was also shown in acute inflammation of skeletal muscle tissue (31), reperfusion injury of kidney medulla (32), and aging of hematopoietic spleen tissue (33). This is the first study that has investigated the fractal dimension of liver lobule and sinusoids in TAA-induced liver injury in both H&E and Masson trichrome stained sections by box-counting method.

TAA-induced liver damage is a widely used animal model of acute liver failure and HE (34–36). Results of tissue samples stained with H&E and Masson's trichrome

showed that TAA caused a decline of the fractal dimension of the liver lobule parenchyma (Fig. 4A). This finding was expected, since our previous research has shown that TAA, in a dose of 600 mg/kg, disrupts lobular architecture of the liver, with loss of laminar hepatocyte organization and extensive fields of necrosis and inflammatory infiltrate (19). Additional histological findings in TAA-exposed liver, which may be responsible for the decline of tissue fractal dimension, include: fatty degeneration, hepatocyte apoptosis, bile duct proliferation, formation of collagen bundles, and infiltration of lymphocytes and macrophages (9, 37, 38). Hepatotoxic effects of TAA are mediated by its toxic intermediates formed by cytochrome P450 oxidase in hepatocytes, which cause liver necrosis, primarily via unstable S-oxide metabolite, thioacetamide-S-dioxide (37, 39). The production of ROS additionally contributes to the liver damage by covalent binding and oxidative modification of liver macromolecules (3, 39).

Fractal analysis performed on liver lobule sinusoids showed that TAA induced an increase in fractal dimension, when compared to the control group in tissue samples stained with H&E (Fig. 4B). This finding may be caused by an increase in the surface of the vascular space, i.e. sinusoids, due to loss of liver parenchyma. Previous studies on TAA-induced liver damage also showed prominent vascular alterations, such as sinusoidal dilatation and congestion and dilated and congested central vein (37, 40) and are in accordance with the present study. Difference between  $D_{sin}$  values in the samples stained with Masson's trichrome showed higher values in the experimental, when compared to the control group. However, statistical difference was at the borderline ( $p = 0.052$ ).

Additionally, both the H&E and Masson's trichrome staining showed that the median  $D_{par}/D_{sin}$  ratio of livers treated with TAA was lower than those of the control group (Fig. 4C). This newly introduced parameter clearly shows that in both experimental staining groups there is a disruption in the relationship between the complexity of parenchyma and sinusoidal space, in terms of the reduction of  $D_{par}$  value and increase in the  $D_{sin}$  val-

ue. Thus, the ratio between the two fractal dimension values of liver compartments provides an additional support to the above mentioned results and therefore may prove useful in future studies dealing with the analysis of liver tissue complexity.

TAA was found to cause HE in a dose-dependent manner. While lower doses (300 mg/kg) cause minimal HE with an increase in EEG alpha band amplitude and proportion, but without significant motor changes, high doses (3x300 mg/kg) cause severe HE with development of hepatic coma (19, 20). The dose of TAA used in the present study (2x300 mg/kg) causes initial motor changes with reduction of motor activity and exploratory behavior in rats, but with preserved vital reflexes (19). Increasing severity of HE is accompanied with more prominent histological changes in the liver, which range from centrilobular and centricentral bridging necrosis in minimal, to extensive necrosis with regenerative response of hepatocytes in severe HE. These and the results of the present study suggest that fractal analysis of liver tissue and sinusoids may be useful not only for quantification of hepatotoxic

effects of TAA, but also possibly in the follow-up of HE. Additionally, TAA increases acetylcholinesterase activity and induces oxidative stress in the brain in a region-specific manner (35, 41). This possibly indicates that fractal dimension of neurons may be also beneficial in the early recognition of TAA-induced HE. The precise correlation between changes in fractal dimension of liver tissue and brain changes should be further evaluated.

The results of our study show that fractal analysis could prove as a useful tool in the quantification of hepatotoxic effect of TAA on the liver tissue. Fractal analysis offers the possibility of describing liver parenchyma and sinusoids quantitatively, which, therefore, gives it the potential of being applied in liver disease diagnostics. The main advantage of this method is that it can evaluate the tissue complexity by using a single parameter, the fractal dimension. Additionally, it offers the possibility of analyzing histological samples stained with standard histological techniques and, thus, it does not require any additional financial.

## References

1. Leise MD, Poterucha JJ, Talwalkar JA. Drug-induced liver injury. *Mayo Clin Proc.* 2014 Jan;89(1):95–106.
2. Devarbhavi H. An Update on Drug-induced Liver Injury. *J Clin Exp Hepatol.* 2012 Sep;2(3):247–59.
3. de David C, Rodrigues G, Bona S, Meurer L, González-Gallego J, Tuñón MJ, et al. Role of quercetin in preventing thioacetamide-induced liver injury in rats. *Toxicol Pathol.* 2011 Oct;39(6):949–57.
4. Panackel C, Thomas R, Sebastian B, Mathai SK. Recent advances in management of acute liver failure. *Indian J Crit Care Med.* 2015 Jan;19(1):27–33.
5. Lee WM, Squires RH, Nyberg SL, Doo E, Hoofnagle JH. Acute liver failure: Summary of a workshop. *Hepatology.* 2008 Apr;47(4):1401–15.
6. Shawcross D, Jalan R. The pathophysiologic basis of hepatic encephalopathy: central role for ammonia and inflammation. *Cell Mol Life Sci.* 2005 Oct;62(19–20):2295–304.
7. Miranda AS de, Rodrigues DH, Vieira LB, Lima CX, Rachid MA, Vidigal PVT, et al. A thioacetamide-induced hepatic encephalopathy model in C57BL/6 mice: a behavioral and neurochemical study. *Arq Neuropsiquiatr.* 2010 Aug;68(4):597–602.
8. Avraham Y, Grigoriadis N, Poutahidis T, Vorobiev L, Magen I, Ilan Y, et al. Cannabidiol improves brain and liver function in a fulminant hepatic failure-induced model of hepatic encephalopathy in mice. *Br J Pharmacol.* 2011 Apr;162(7):1650–8.
9. Luo M, Dong L, Li J, Wang Y, Shang B. Protective effects of pentoxifylline on acute liver injury induced by thioacetamide in rats. *Int J Clin Exp Pathol.* 2015;8(8):8990–6.
10. Tambasco M, Costello BM, Kouznetsov A, Yau A, Magliocco AM. Quantifying the architectural complexity of microscopic images of histology specimens. *Micron.* 2009 Jun;40(4):486–94.
11. Zaletel I, Ristanović D, Stefanović BD, Puškaš N. Modified Richardson's method versus the box-counting method in neuroscience. *J Neurosci Methods.* 2015 Mar 15;242:93–6.
12. Puškaš N, Zaletel I, Stefanović BD, Ristanović D. Fractal dimension of apical dendritic arborization differs in the superficial and the deep pyramidal neurons of the rat cerebral neocortex. *Neurosci Lett.* 2015 Mar 4;589:88–91.
13. Di Ieva A, Grizzi F, Jelinek H, Pellionisz AJ, Losa GA. Fractals in the Neurosciences, Part I: General Principles and Basic Neurosciences. *Neuroscientist.* 2014 Aug;20(4):403–17.
14. Moal F, Chappard D, Wang J, Vuillemin E, Michalak-Provost S, Rousselet MC, et al. Fractal dimension can distinguish models and pharmacologic changes in liver fibrosis in rats. *Hepatology.* 2002 Oct;36(4 Pt 1):840–9.
15. Dioguardi N, Grizzi F, Franceschini B, Bossi P, Russo C. Liver fibrosis and tissue architectural change measurement using fractal-rectified metrics and Hurst's exponent. *World J Gastroenterol.* 2006 Apr 14;12(14):2187–94.
16. de Arruda PFF, Gatti M, Facio FN, de Arruda JGF, Moreira RD, Murta LO, et al. Quantification of fractal dimension and Shannon's entropy in histological diagnosis of prostate cancer. *BMC Clin Pathol.* 2013 Feb 18;13:6.
17. Cross SS. Fractals in pathology. *J Pathol.* 1997 May;182(1):1–8.
18. Bianciardi G. Differential Diagnosis: Shape and Function, Fractal Tools in the Pathology Lab. *Nonlinear Dynamics Psychol Life Sci.* 2015 Oct;19(4):437–64.
19. Mladenović D, Radosavljević T, Hrnčić D, Rašić-Marković A, Puškaš N, Maksić N, et al. Behavioral and electroencephalographic manifestations of thioacetamide-induced encephalopathy in rats. *Can J Physiol Pharmacol.* 2012 Sep;90(9):1219–27.
20. Mladenovic D, Hrnčić D, Rasić-Marković A, Puskas N, Petrovich S, Stanojlović O. Spectral analysis of thioacetamide-induced electroencephalographic changes in rats. *Hum Exp Toxicol.* 2013 Jan;32(1):90–100.
21. Milosević NT, Ristanović D, Jelinek HF, Rajković K. Quantitative analysis of dendritic morphology of the  $\alpha$  and  $\delta$  retinal ganglion cells in the rat: a cell classification study. *J Theor Biol.* 2009 Jul 7;259(1):142–50.
22. Mandelbrot BB. *The Fractal Geometry of Nature*. Updated and Augmented edition. San Francisco: W.H. Freeman &

- Co Ltd; 1982. 460 p.
23. Losa GA, Ristanović D, Ristanović D, Zaletel I, Beltraminelli S. From Fractal Geometry to Fractal Analysis. *Applied Mathematics*. 2016 Mar 10;07(04):346.
  24. Falconer K. *Fractal Geometry: Mathematical Foundations and Applications*. 2 edition. Chichester, England: Wiley; 2003. 366 p.
  25. Smith TG, Lange GD, Marks WB. Fractal methods and results in cellular morphology--dimensions, lacunarity and multifractals. *J Neurosci Methods*. 1996 Nov;69(2):123–36.
  26. Losa GA. Fractals and their contribution to biology and medicine. *Medicographia*. 2012;34:365–74.
  27. Gaudio E, Chaberek S, Montella A, Pannarale L, Morini S, Novelli G, et al. Fractal and Fourier analysis of the hepatic sinusoidal network in normal and cirrhotic rat liver. *J Anat*. 2005 Aug;207(2):107–15.
  28. Streba CT, Pirici D, Vere CC, Mogoantă L, Comănescu V, Rogoveanu I. Fractal analysis differentiation of nuclear and vascular patterns in hepatocellular carcinomas and hepatic metastasis. *Rom J Morphol Embryol*. 2011;52(3):845–54.
  29. Pantic I, Petrovic D, Paunovic J, Vucevic D, Radosavljevic T, Pantic S. Age-related reduction of chromatin fractal dimension in toluidine blue - stained hepatocytes. *Mech Ageing Dev*. 2016 Jul;157:30–4.
  30. Fabrizii M, Moinfar F, Jelinek HF, Karperien A, Ahammer H. Fractal analysis of cervical intraepithelial neoplasia. *PLoS ONE*. 2014;9(10):e108457.
  31. Stankovic M, Pantic I, De Luka SR, Puskas N, Zaletel I, Milutinovic-Smiljanic S, et al. Quantification of structural changes in acute inflammation by fractal dimension, angular second moment and correlation. *J Microsc*. 2016 Mar;261(3):277–84.
  32. Pantic I, Nestic Z, Paunovic Pantic J, Radojević-Škodrić S, Cetkovic M, Basta Jovanovic G. Fractal analysis and Gray level co-occurrence matrix method for evaluation of reperfusion injury in kidney medulla. *J Theor Biol*. 2016 May 21;397:61–7.
  33. Pantic I, Paunovic J, Basta-Jovanovic G, Perovic M, Pantic S, Milosevic NT. Age-related reduction of structural complexity in spleen hematopoietic tissue architecture in mice. *Exp Gerontol*. 2013 Sep;48(9):926–32.
  34. Rahman TM, Hodgson HJF. Animal models of acute hepatic failure. *Int J Exp Pathol*. 2000 Apr;81(2):145–57.
  35. Mladenović D, Krstić D, Colović M, Radosavljević T, Rasić-Marković A, Hrnčić D, et al. Different sensitivity of various brain structures to thioacetamide-induced lipid peroxidation. *Med Chem*. 2012 Jan;8(1):52–8.
  36. Mladenović D, Hrnčić D, Petronijević N, Jevtić G, Radosavljević T, Rašić-Marković A, et al. Finasteride improves motor, EEG, and cellular changes in rat brain in thioacetamide-induced hepatic encephalopathy. *Am J Physiol Gastrointest Liver Physiol*. 2014 Nov 1;307(9):G931–940.
  37. Saleh DO, Abdel-Jaleel GAR, El-Awdan SA, Oraby F, Badawi M. Thioacetamide-induced liver injury: protective role of genistein. *Can J Physiol Pharmacol*. 2014 Nov;92(11):965–73.
  38. Lim S, Lee S-J, Nam K-W, Kim KH, Mar W. Hepatoprotective effects of reynosin against thioacetamide-induced apoptosis in primary hepatocytes and mouse liver. *Arch Pharm Res*. 2013 Apr;36(4):485–94.
  39. Porter WR, Neal RA. Metabolism of thioacetamide and thioacetamide S-oxide by rat liver microsomes. *Drug Metab Dispos*. 1978 Aug;6(4):379–88.
  40. Hassan H, Serag H, Abdel-Hamid N, Amr M. Synergistic curative effect of chicory extract and cisplatin against thioacetamide-induced hepatocellular carcinoma. *Hepatoma Research*. 2015;1(3):147.
  41. Mladenović D, Petronijević N, Stojković T, Velimirović M, Jevtić G, Hrnčić D, et al. Finasteride Has Regionally Different Effects on Brain Oxidative Stress and Acetylcholinesterase Activity in Acute Thioacetamide-Induced Hepatic Encephalopathy in Rats. *PLoS One*. 2015 Aug 4;10(8).